Isothermal section of the ternary phase diagram U–Fe–Ge at 900 °C and its new intermetallic phases

M. S. Henriques, David Berthebaud, A. Lignie, Z. El Sayah, C. Moussa, O. Tougait, L. Havela, A. P Gonçalves

Isothermal section of the ternary phase diagram U-Fe-Ge at 900ºC and its new intermetallic phases

M. S. Henriques[1,2*], D. Berthebaud[3§], A. Lignie[3], Z. El Sayah[3], C. Moussa[3], O. Tougait[3], L. Havela[4], A.P Gonçalves[2]

[1]*Institute of Physics, Academy of Sciences of the Czech Republic, Na Slovance 2, 182 21 Prague, Czech Republic*

[2]*CCTN, IST/CFMCUL, University of Lisbon, Nuclear and Technological Campus, P-2695-066 Bobadela, Portugal*

[3]*Institut des Sciences Chimiques de Rennes, Chimie du Solide et Matériaux, Université Rennes 1, UMR CNRS 6226, 263 Avenue du Général Leclerc, 35042 Rennes, France*

[4]*Department of Condensed Matter Physics, Faculty of Mathematics and Physics, Charles University, Ke Karlovu 5, 121 16 Prague, Czech Republic*

[§] *Present address: CRISMAT, UMR CNRS 6508, 6 bd. Maréchal Juin, 14050 Caen, France*

*Corresponding author: mish@itn.pt (M. Henriques)

Abstract

The isothermal section at 900ºC of the U-Fe-Ge ternary system was assessed using experimental results from X-ray diffraction and observations by scanning electron microscopy coupled with energy dispersive X-ray spectroscopy chemical analysis. The phase diagram at this temperature is characterized by the formation of fourteen stable phases: four homogeneity ranges and ten intermetallic compounds. Among these, there is an extension of the binary compound UFe_2 into the ternary system ($UFe_{2-x}Ge_x$, $x < 0.15$), three ternary line compounds, $U_2Fe_{17-x}Ge_x$ ($2 < x < 3.7$), $UFe_{1-x}Ge_2$ ($0.58 < x < 0.78$), $UFe_{6+x}Ge_{6-x}$ ($x < 0.7$), and ten ternary compounds, U_2Fe_3Ge, $U_6Fe_{16}Ge_7$, UFe_4Ge_2, $U_6Fe_{22}Ge_{13}$, $UFeGe$, $U_3Fe_4Ge_4$, UFe_2Ge_2, $U_{34}Fe_{3.32}Ge_{33}$, $U_3Fe_2Ge_7$, and $U_9Fe_7Ge_{24}$.

Keywords: A. Actinides alloys and compounds; B. Crystal structure; C. X-ray diffraction.

1. Introduction

The study of phase diagrams provides important information about the formation and stability of new compounds and the phase relations, being a good base for the knowledge of properties and development of original materials. Research in ternary systems of the type (*f* element)-(*d* element)-(*p* element) is a good example. Usually, the *p* and *d* elements have an important role in the delocalization of the *f* electrons and, in addition, the *p* element can introduce interesting properties, such as enhancement of the Seebeck coefficient. Systems containing an *f* element, iron, and germanium were intensively studied for the lanthanides due to the discovery of the giant magnetocaloric effect in pseudo-binary compounds such as $Gd_5Si_xGe_{4-x}$, or in similar systems when substituting Si and Ge by other non-metals or transition metals [1,2]. So far, ternary systems of the type *R*-Fe-Ge are reported for *R* = La, Ce, Nd, Sm, Eu, Gd, Tb, Dy, Ho, Er, Tm, and Yb [1,3,4]. For actinide-containing systems, a more systematic search was started 25 years ago and many theoretically types of behavior or new physical effects were experimentally identified in uranium ternary intermetallic compounds [5-7].

Isothermal sections for uranium systems of the type U-Fe-*X* were already reported for *X* = B [8], Al [9], Si [10], Sn [11], and Ga [12]. Preliminary results on the isothermal section of the U-Fe-Ge at 900ºC were reported [13], the systematic study of this system revealing a rich variety of new compounds. In this framework, the ternary compounds U_2Fe_3Ge [14,15], $U_9Fe_7Ge_{24}$ [16], $U_3Fe_4Ge_4$ [17,18], $U_{34}Fe_{4-x}Ge_{33}$ [19] and $U_3Fe_2Ge_7$ **[**20**]** were already described. Here we present results of the methodical investigation assessing the isothermal section of the ternary phase diagram U-Fe-Ge at 900ºC, which was supported in experimental results from X-ray diffraction and scanning electron microscopy coupled with energy-dispersive spectroscopy.

2. Literature data

2.1 Binary systems

For the binary systems U-Fe, U-Ge and Fe-Ge in total 10 binary compounds and one solid solution have been reported in literature. The U-Fe diagram is well studied [21] and only two binary compounds, having small solubility ranges, are formed. Nevertheless, at *T* = 900ºC only UFe_2 ($MgCu_2$-type) is stable, after the peritectic decomposition of U_6Fe (U_6Mn-type) at 805ºC. At 900ºC there is a liquid phase in the U-Fe binary diagram for compositions between 12 and 40 at.% of iron. The solubility of Fe in γ-U is about 4 atomic percent (at.%) at this temperature. For

the U-Ge binary system [22], five compounds, each without significant solubility range, were found to be stable at 900ºC, namely UGe_3, UGe_2, U_3Ge_5, UGe, and U_5Ge_4. At this temperature, the solubility of Ge in γ-U is around 1 at.%. A high temperature phase, UGe_{2-x} with the $ThSi_2$-defect type is claimed to exist at elevated temperature only [23]. The Fe-Ge system [21] shows four stable binary phases at 900ºC: $Fe_{13}Ge_3$, Fe_3Ge, $Fe_{3.2}Ge_2$, and $Fe_{13}Ge_8$. The Fe_3Ge compound has two polymorphic forms, the hexagonal Ni_3Sn- type being the stable form between 700ºC and 1122ºC. In this system an α-solid solution corresponding to the solubility of Ge in iron up to 17.5 at.% at 900ºC was identified. It is also important to note that at this temperature there is a liquid zone for germanium content between 65 and 86 at.%. The relevant crystallographic and thermodynamic data on unary and binary phases taken from the three binary boundary systems relevant to this work are gathered in Table 1.

2.1 Ternary phases

In the ternary system U-Fe-Ge one intermediate solid-solution and eight intermetallic compounds are known so far. Chevalier and co-authors investigated the homogeneity range $U_2Fe_{17-x}Ge_x$ and reported it as crystallizing in the Th_2Ni_{17} structure-type (*P*6_3*/mmc*) and stable for $2 < x < 3$ at 850ºC [24]. According to Canepa *et al.* [25], the UFeGe compound crystallizes in an orthorhombic lattice (*Pnma*) with the structure type TiNiSi above 500K. At this temperature, it undergoes a structural transition to its own monoclinic (*P*2_1*/m*) type. UFe_2Ge_2 was found to crystallize with the structure-type $ThCr_2Si_2$ (*I4/mmm*) [26], and UFe_6Ge_6 belongs to the hexagonal (*P6/mmm*) YCo_6Ge_6-type [27]. The compound U_2Fe_3Ge crystallizes in the hexagonal Mg_2Cu_3Si structure, an ordered variant of the $MgZn_2$ Laves structure (C14) [14,15,28]. The formation of the compound $U_9Fe_7Ge_{24}$ was reported as having an original tetragonal structure (space group *I4/mmm*) [16]. $U_3Fe_4Ge_4$ was recently identified as crystallizing in the orthorhombic $Gd_3Cu_4Ge_4$ structure type [17,18]. Another novel ternary phase $U_{34}Fe_{4-x}Ge_{33}$ with $x = 0.68$ has also been synthesized. It crystallizes in its own tetragonal structure type, which can be described as derived from the the binary USi ($U_{34}Si_{34.5}$ structure-type, space group *I*4/*mmm*) [16]. The last reported compound in this system is $U_3Fe_2Ge_7$ **[**20**]**. Single crystal studies have revealed that $U_3Fe_2Ge_7$ crystallizes in the orthorhombic isotype $La_3Co_2Sn_7$. The reported crystal structure and lattice parameters data for the ternary phases can be found in Table 1.

3. Experimental

In the present study, polycrystalline samples of composition xU:yFe:zGe were prepared by melting the calculated amounts of the elements (purity > 99.99%) in arc or induction furnaces, under a high purity argon atmosphere. The uranium lumps were cleaned in diluted nitric acid prior to melting. To ensure better homogeneity, the samples were melted at least three times. The weight losses were smaller than 1% (for samples with mass lower than 0.3 g). The annealing was carried out on ingots wrapped in Mo foil, encapsulated in evacuated and flame-sealed silica tubes, at T = 900ºC for 4 weeks. The samples were then water-quenched to room temperature. Phase analysis was performed using X-ray powder diffraction and scanning electron microscopy (SEM) coupled with energy-dispersive X-ray spectroscopy (EDS).

X-ray diffraction patterns were collected at room temperature in fine powdered samples using Co Kα radiation on an Inel CPS 120 diffractometer, equipped with a position-sensitive detector, and using Cu Kα radiation on a Philips automated diffractometer PW 1710. The step size was 0.03º in the angular 2θ range 10-90º. The diffraction patterns were first compared with the calculated ones using the PowderCell software [29], and the Rietveld refinements were performed with the help of FullProf [30]. An experimentally determined $K\alpha_1/K\alpha_2$ intensity ratio of 0.5, a factor cos θ = 0.7998 for the monochromator polarization correction and a Pseudo-Voigt profile shape function were used. The background was manually refined and introduced in the input file.

Single crystal X-ray diffraction data were collected on selected crystals at room temperature in a Bruker Kappa CCD four circle diffractometer working with MoKα radiation (λ = 0.71073 Å). The orientation matrix and the unit-cell parameters were derived from the first ten measured frames of the data using the DENZO software [31]. The scaling and merging of redundant measurements of the different data sets as well as the cell refinement was performed using DENZO-ScalePack [32]. Semi-empirical absorption corrections were made by the MULTISCAN software [33]. Structural models were determined by direct methods using SIR-97 [34]. All structure refinements and Fourier syntheses were made with the help of SHELXL-97 [35]. The atomic positions have been standardized using STRUCTURE TIDY [36].

The microstructure of polished samples was analyzed using a Jeol-JSM 6400 scanning SEM equipped with an EDS Oxford Link-Isis Si-Li analyzer and an analytical FEG-SEM Jeol 7001F

coupled with Oxford light elements EDS detector. At least three analysis points were acquired for each phase. The EDS software package performed automated matrix corrections. Binary or ternary compounds, unequivocally identified by X-ray diffraction, and without significant solubility ranges, were previously used as standards to obtain a more accurate chemical composition of the phases. Figure 1 presents all the prepared nominal compositions in the Gibbs triangle together with the number of phases found in each sample after the annealing at 900°C in the above mentioned conditions. Results of XRD and SEM-EDS analysis for selected samples (marked in Fig. 1) are compiled in Table 2.

4. Results and discussion

The ternary U-Fe-Ge isothermal section at 900ºC, built after the results of X-ray diffraction and SEM-EDS analysis, is shown in Fig. 2. The crystallographic data for the ternary compounds and homogeneity ranges found within the present study of the U-Fe-Ge system at 900ºC are presented in Table 3.

The existence and composition of all the U-Ge and Fe-Ge binary compounds known to be stable at 900ºC was confirmed and their composition and crystal structure are in agreement with the literature data. The UGe_{2-x} phase was not found to be stable at this temperature. All the binary compounds belonging to these two systems have negligible extension into the ternary system (within the EDS detection edge). The limits of the solubility range for the α solid solution (~ 18.2 at.% of Ge) and the liquid region *L*2 (between 65 and 87 at.% of Ge) in the Fe-Ge system [21] were corroborated by the present work, giving 17.8 at.% of Ge and 65.3 at.% of Fe, respectively. Moreover, no signs of significant extension of *L*2 into the ternary phase diagram were detected during the present work. It is worth to note that the binary compounds $Fe_{13}Ge_8$ and $Fe_{3.2}Ge_2$ were distinguished in two different samples (samples 16 and 18, respectively, Table 2 and Figure 2) based on the SEM-EDS analysis together with X-ray diffraction results, since the very close chemical composition of both phases would not allow a clear distinction between them only by backscattered electrons imaging and EDS. At 900ºC the solubility of Fe in γ-U was estimated to be ≈ 4 at.% and agrees well with the binary diagram data [21]. The binary limits of the liquid region *L*1 in the ternary diagram are also in accordance with the literature data (~12 to 40 at.% of Fe). Nevertheless, *L*1 extends into the ternary diagram at 900°C, having its maximum for about 3.35 at.% of Ge. In the U-Fe system at 900ºC, the binary compound UFe_2 (the only

compound stable at this temperature) shows an extension into the ternary system as a solubility range $UFe_{2-x}Ge_x$ (*A*), due to the substitution of Fe by Ge up to 5 at.%.

The ternary line compound $U_2Fe_{17-x}Ge_x$ (*B*) adopting the Th_2Ni_{17} structure-type is stable at 900ºC, as already mentioned. Nevertheless, the evaluated range at this temperature ($2 < x < 3.7$) is slightly larger than the one previously announced after annealing at 850ºC ($2 < x < 3$) [24]. It was known that the homogeneity range of the compound UFe_6Ge_6 should be small [27]. Indeed, during this work it was found that its hexagonal structure is still stable when substituting Ge by Fe up to 5.8 at.%, forming a ternary line compound $UFe_{6+x}Ge_{6-x}$ for $x < 0.8$ at 900ºC (*J*).

Among the ternary stoichiometric compounds previously reported, all of them were found to be stable at 900°C: U_2Fe_3Ge (*C*), UFeGe (*G*), $U_3Fe_4Ge_4$ (*H*), UFe_2Ge_2 (*I*), $U_{34}Fe_{3.32}Ge_{33}$ (*K*), $U_3Fe_2Ge_7$ (*M*), and $U_9Fe_7Ge_{24}$ (*N*). The crystal data obtained in the present work from Rietveld or single crystal refinements for each one of these phases is presented in Table 3.

The hexagonal C14 Laves phase U_2Fe_3Ge (*C*) was first found in a sample with composition 28U:54Fe:18Ge (Fig. 3) and the crystalline data obtained are in agreement with the previous works (Tables 1 and 3) [14,15,28]. This compound crystallizes in the Mg_2Cu_3Si structure type, which is a ternary ordered variant of the $MgZn_2$ structural archetype. In U_2Fe_3Ge nearest U-U distances are ~2.75 Å and it orders ferromagnetically below 55 K [14,15,28].

UFeGe (*G*) and UFe_2Ge_2 (*I*) have been observed in this study and the structural analysis matches the literature data (Tables 1 and 3); further there is no evidence of significant solubility in the solid state. The 1:1:1 compound was found present in both polymorphic forms. Apparently the martensitic transformation (structural phase transition into the monoclinic phase) cannot be avoided when quenching, but strains do not allow finishing it entirely.

From the analysis of a well crystallized sample with stoichiometry 3U:4Fe:4Ge prepared by arc-melting the compound $U_3Fe_4Ge_4$ (*H*) was found (Fig. 4). The Rietveld refinement following the powder data collection showed that this new phase crystallizes in the orthorhombic structure-type $Gd_3Cu_4Ge_4$ (*Immm* space group) and has as lattice parameters $a = 4.086(5)$ Å, $b = 6.640(5)$ Å, and $c = 13.686(5)$ Å. This compound orders ferromagnetically below the Curie temperature $T_C = 18$ K [17,18].

The compound $U_{34}Fe_{3.32}Ge_{33}$ (*K*) was first identified in an as-cast sample with nominal composition 9U:Fe:10Ge and later confirmed on stoichiometric samples (Fig. 5). The crystal structure determination, using X-ray diffraction data collected on $U_{34}Fe_{4-x}Ge_{33}$ (x=0.68) single

crystals, indicated an original tetragonal structure type (space group *I4/mmm*) [19] that can be seen as a derivative of the binary USi [37]. The lattice parameters at room temperature are a = 10.875(5) Å and c = 25.250(5) Å. Magnetic measurements have revealed a ferromagnetic-type transition at 28 K [19].

The compound $U_3Fe_2Ge_7$ (*M*) was found after EDS analysis of an annealed sample with nominal composition U:0.75Fe:2Ge (Fig. 6), which exhibited an X-ray powder pattern with unindexed reflections. $U_3Fe_2Ge_7$ crystallizes within the orthorhombic *Cmmm* space group as an isotype of $La_3Co_2Sn_7$. The cell parameters a = 4.153(1) Å, b = 24.927(1) Å, and c = 4.155(1) Å were found after refinement of X-ray diffraction data collected from a powdered sample. $U_3Fe_2Ge_7$ is probably formed through peritectic or peritectoid solid state reaction, since this phase is not present in as-cast samples with the composition ratio 3U:2Fe:7Ge, appearing only in the sequence of annealing procedures. Nevertheless, single crystals were grown by the flux method and studies of electronic properties have shown that the compound orders ferromagnetically at 62 K [20].

The formation of the compound $U_9Fe_7Ge_{24}$ (*N*) was evidenced by X-ray diffraction patterns and EDS analysis performed on samples with composition ratio U:Fe:3Ge annealed at 900ºC (Fig. 7). $U_9Fe_7Ge_{24}$ crystallizes in its own structure type within the tetragonal space group *I4/mmm* and the lattice parameters were found to be a = 12.365(1) Å and c = 18.256(3) Å, in good agreement with the previous work [16]. This compound is a paramagnet down to 2 K.

In addition to these phases, the isothermal section of the ternary system U-Fe-Ge at 900ºC presents four new stable phases: $U_6Fe_{16}Ge_7$ (*D*), UFe_4Ge_2 (*E*), $U_6Fe_{22}Ge_{13}$ (*F*), and $UFe_{1-x}Ge_2$ (*L*).

The compound $U_6Fe_{16}Ge_7$ (*D*) was identified in a polycrystalline sample with composition 28U:54Fe:18Ge (Fig. 3). This phase was always found in annealed samples and mixed with other phases. Thus, so far all the obtained powder X-ray diffraction patterns were of insufficient quality for a full structural Rietveld analysis. Nevertheless, the lattice constant was successfully obtained as a = 11.923(6) Å by analogy with the structural archetype $Mg_6Cu_{16}Si_7$ (space group $Fm\bar{3}m$). This crystal structure is a ternary ordered variant of the Th_6Mn_{23}-type structure, which can accommodate interstitial elements in octahedral cages formed by uranium atoms, as it was demonstrated for C insertion in the lattice of the silicon analogue compound, $U_6Fe_{16}Si_7$ [38].

The presence of the phase UFe_4Ge_2 (*E*) was verified for the first time after heat treatment at 900ºC of a sample with composition 1U:6Fe:3Ge and later confirmed in an alloy with nominal composition 12U:60Fe:28Ge. Majority of the reflections in the X-ray diffraction patterns (Fig. 8) matched the tetragonal isotype $ZrFe_4Si_2$ (space group $P4_2/mnm$) and the refined lattice parameters were a = 7.274(4) Å and c = 3.884(3) Å. Details of data collection and structure refinement are given in Table 4, whereas atomic positions and isotropic displacement parameters can be found in Table 5. The interatomic distances are presented in Table 6. The unit cell of UFe_4Ge_2 is shown in Fig. 9. In this structure all atoms are located in mirror planes, which are perpendicular to the fourfold axis, and it may be viewed as a body-centered array of U atoms. Each U atom has the coordination number, CN = 20. It is surrounded by six Ge atoms forming a quasi-regular octahedron. The coordination sphere of U includes two other U atoms at distances of 3.85 Å. The Fe atoms have coordination number 12 and as near neighbors three Ge atoms in a pseudo-triangular coordination and each Ge atom (CN = 9) is in the center of a tricapped trigonal prism. Interestingly, some rare earth compounds crystallizing within this structure were found to be ferromagnetic quasi-one-dimensional heavy fermion metals [39].

UFe_4Ge_2 was found in equilibrium with an unidentified phase in an as-cast sample with initial composition 1U:6Fe:3Ge. After induction furnace heat treatment of this sample the second phase was well crystallized. A suitable crystal was analyzed by X-ray diffraction showing that this phase was $U_6Fe_{22}Ge_{13}$ (*F*) crystallizing within the orthorhombic space group *Pbam*, with lattice parameters a = 12.674(5) Å, b = 24.196(5) Å, and c = 4.005(5) Å. The crystal characteristics along with the intensity data collection and structural resolution are presented in Table 7, while atomic coordinates and isotropic displacement parameters are given in Table 8. The interatomic distances can be found in Table 9. This new structure-type has 21 independent lattice sites with complex coordination spheres. The unit cell of $U_6Fe_{22}Ge_{13}$ is shown in Fig. 10, together with the coordination polyhedra for the three nonequivalent positions for U atoms in the structure. U1 atom is surrounded by 18 atoms which form an irregular hexagonal prism. A comparable coordination polyhedron is found for U2 and U3 although these atoms are coordinated by 17 atoms. None of them has other U atoms as nearest neighbors, the shortest inter-uranium distance coinciding with the lattice parameter c = 4.00 Å. A scanning electron micrograph of this phase in equilibrium with UFe_2Ge_2 and Fe_3Ge is presented in Fig. 11.

The new ternary line compound (*L*) $UFe_{1-x}Ge_2$ with $0.58 < x < 0.78$, was found to crystallize in the deficient orthorhombic structure type $CeNi_{1-x}Si_2$. The refinement of single crystal X-ray lead to the lattice parameters a = 4.083(5) Å, b = 15.805(5) Å, and c = 4.030(5) Å (for x = 0.6). Details of data collection and refinement procedures can be found in Table 10, whereas the atomic coordinates and isotropic displacement parameters are presented in Table 11 and selected interatomic distances are listed in Table 12. The $CeNiSi_2$ –type is a well known structural archetype and it is characterized by infinite chains of trigonal prisms formed by the *f* atoms, in this case the uranium atoms. A view of the unit cell is shown in Fig. 12. In this structure the U atoms have CN = 19, including two U atoms at a distance 3.86 Å. Another feature of this structure type is the non-stoichiometry in the 4*c* site of the 3*d* metal, which in most cases allows the formation of a solubility range. For the sample with composition $UFe_{0.4}Ge_2$, the occupation of the 4*c* site is 40%. The high residual electronic density in the Fourier maps (Table 10) and of the isotropic displacement parameters for the atoms Fe1 and Ge2 (Table 11) might be related with the crystallographic disorder due to the low occupation of the Fe site. The interatomic distance Fe1-Ge2 is 2.19 Å (Table 12).

A remarkable feature of the 900ºC isothermal sections of ternary systems U-Fe-*X* (*X* = Al, Si, Ga, Ge) is the number of intermetallic phases formed: in U-Fe-Ge ten compounds and four solid solutions are stable at this temperature. The U-Fe-Si has nine reported stable compounds and four intermediate phases at 900ºC [11]. For the U-Fe-Ga [13] and U-Fe-Al [10] systems, the degree of substitution between iron and gallium or aluminium is the outstanding aspect and the consequence is the high stability of six homogeneity ranges, which can be found in each one of the respective isothermal sections. In all these systems, the most stable homogeneity ranges are of binary types (such as $ThMn_{12}$ or Th_2Ni_{17}), which do not exist in the binary diagram U-Fe but can be stabilized by the addition of the *p* element. Concerning the solubility of binary compounds in ternary phase diagrams, UFe_2 is the only compound showing significant solubility, and its $MgCu_2$ structure-type allocates Ge, Ga, and Al, but not Si in the lattice as Fe substitute. The systems U-Fe-Ge and the U-Fe-Si exhibit numerous similarities. They share a homogeneity range with Th_2Ni_{17}-type, even though the solubility range is somewhat more extended for germanium, indicating a higher stability for this element. Equally, in both systems there is an equiatomic compound: UFeSi crystallizes in the structure-type TiNiSi, however for UFeGe this structure is only stable above 227ºC. Other composition ratios mutually shared within these

systems (crystallizing in the same structure-type in both diagrams) are 1:2:2, 2:3:1, 6:16:7, and 3:2:7.

5. Conclusions

The ternary U-Fe-Ge section at 900ºC was experimentally investigated and the equilibrium domains have been established. It is characterized by the formation of ten ternary intermetallic compounds and four significant solubility ranges. All the previously reported binary and ternary phases have been confirmed and their crystallographic analysis is in agreement with the literature. Moreover, from the whole set of binary compounds only UFe_2 extends into the ternary diagram at 900°C, forming $UFe_{2-x}Ge_x$ with $x < 0.15$. From those already known ternary stoichiometric compounds (U_2Fe_3Ge, UFeGe, $U_3Fe_4Ge_4$, UFe_2Ge_2, UFe_6Ge_6, $U_{34}Fe_{3.32}Ge_{33}$, $U_3Fe_2Ge_7$ and $U_9Fe_7Ge_{24}$), only UFe_6Ge_6 forms a ternary line compound ($UFe_{6+x}Ge_{6-x}$ with $x < 0.8$). The ternary line compound $U_2Fe_{17-x}Ge_x$ is stable at 900ºC for $2 < x < 3.7$. In addition, three new compounds and a ternary line compound were discovered: $U_6Fe_{16}Ge_7$, UFe_4Ge_2, $U_6Fe_{22}Ge_{13}$ and $UFe_{1-x}Ge_2$ with $0.58 < x < 0.78$. The crystal structures of $U_6Fe_{16}Ge_7$, UFe_4Ge_2 and $UFe_{1-x}Ge_2$ were confirmed to belong to known crystalline archetypes, whereas $U_6Fe_{22}Ge_{13}$ crystallizes in an original orthorhombic structure (space group *Pbam*).

Acknowledgments

M. Henriques acknowledges the support of the Portuguese Foundation for Science and Technology through the grant SFRH/BD/66161/2009. This work was also supported by the exchange Program CNRS/FCT (PICS SCR-ITN) 2011–2013. The authors acknowledge the use made of the Nonius Kappa CCD diffractometer through the Centre de Diffraction X de l'Université de Rennes1 (CDIFX). We also thank the Centre de Microscopie Électronique à Balayage et microAnalyse (CMEBA) for the EDS analysis.

References

[1] Y.H. Zhuang, C.H. Ma, K.F. Li, X. Chen, *J. Alloys. Compd.* 467 (2009) 154.

[2] Y.H. Zhuang, W.D. Huang, J.Q. Li, Y.X. Jian, J.L. Huang, *J. Alloys. Compd.* 414 (2006) 151.

[3] P. Salamakha, M. Konyk, O. Sologub, O. Bodak, *J. Alloys. Compd.* 234 (1996) 151.

[4] Y.H. Zhuang, X. Chen, J.L. Yan, K.F. Li, C.H. Ma, *J. Alloys. Compd.* 465 (2008) 216.

[5] N.T. Huy, A. Gasparini, D.E. de Nijs, Y. Huang, J.C.P. Klaasse, T. Gortenmulder, A. de Visser, A. Hamann, T. Görlach, H. von Löhneysen, *Phys. Rev. Lett.* 99 (2007) 067006.

[6] D. Aoki, A.D. Huxley, E. Ressouche, D. Braithwaite, J. Flouquet, J.P. Brison, E. Lhotel, C. Paulsen, *Nature* 413 (2001) 613.

[7] T.T.M. Palstra, A.A. Menovsky, J. van den Berg, A.J. Dirkmaat, P.H. Kes, G.J. Nieuwenhuys, J.A. Mydosh, Phys. Rev. Lett. 55 (1985) 2727.

[8] M. Dias, P.A. Carvalho, O. Sologub, O. Tougait, H. Noël, C. Godart, E. Leroy, A.P. Gonçalves, *Intermetallics* 15 (2007) 413.

[9] A.P. Gonçalves, H. Noël, *Intermetallics* 13 (2005) 580.

[10] D. Berthebaud, O.Tougait, A.P. Gonçalves, H. Noël, *Intermetallics* 16 (2008) 373.

[11] A.P. Gonçalves, H. Noël, *Intermetallics* 9 (2001) 473.

[12] A.P. Gonçalves, H. Noël, O. Tougait, A. Zelinskiy, *Proceedings of the 38 JDA,* Wroclaw, Poland, 2008, P06.

[13] D. Berthebaud, *'Synthèse, Structure Cristalline et Propriétés Electroniques des Composés Intermétalliques Dans les Systèmes Ternaires (U-Ce)-Fe-(Ge,Si)'*, PhD Thesis, Université de Rennes 1 (2007).

[14] M.S. Henriques, O. Tougait, H. Noël, L.C.J. Pereira, J.C. Waerenborgh, A.P. Gonçalves, *Solid State Commun.* 148 (2008) 159.

[15] M.S. Henriques, D.I. Gorbunov, J.C. Waerenborgh, L. Havela, A.B. Shick, M. Diviš, A.V. Andreev, A.P. Gonçalves, *J. Phys.: Condens. Matter* 25 (2013) 066010.

[16] M.S. Henriques, D. Berthebaud, L.C.J. Pereira, E.B. Lopes, M.B.C. Branco, H. Noël, O. Tougait, E. Šantavá, L. Havela, P.A. Carvalho, A.P. Gonçalves, *Intermetallics* 19 (2011) 841.

[17] D. Berthebaud, O. Tougait, M. Potel, E.B. Lopes, J.C. Waerenborgh, A.P. Gonçalves, H. Noel, *J. Alloys Compd.* 554 (2013) 408.

[18] M.S. Henriques, D.I. Gorbunov, J.C. Waerenborgh, L. Havela, A.V. Andreev, Y. Skourski, A.P. Gonçalves, *J. Alloys Compd*. 555 (2013) 304.

[19] M.S. Henriques, D. Berthebaud, J.C. Waerenborgh, E.B. Lopes, M. Pasturel, O. Tougait, A.P. Gonçalves, *J. Alloys Compd.* 606 (2014) 154.

[20] M.S. Henriques, D.I. Gorbunov, J.C. Waerenborgh, M. Pasturel, A.V. Andreev, M. Dušek, Y. Skourski, L. Havela, A.P. Gonçalves, *in preparation* (2015).

[21] O. Kubaschewski, *Iron-Binary Phase Diagrams*, Berlin: Springer-Verlag, 1982, p. 160.

[22] T.B Massalski, H. Okamoto, P.R. Subramanian, L. Kacprzak (Eds.) *Binary alloy phase diagrams*, 2nd ed, vol.1-3, ASM International, 1990.

[23] R. Troc, H. Noël, P. Boulet, Philo. Mag. Part B. 82 (2002) 205.

[24] B. Chevalier, P. Gravereau, T. Berlureau, L. Fournès, J. Etourneau, *J. Alloys Compd.* 233 (1996) 174.

[25] F. Canepa, P. Manfrinetti, M. Pani, A. Palenzona, *J. Alloys Compd.* 234 (1996) 225.

[26] R. Marazza, R. Ferro, G. Rambaldi, G. Zanicchi, *J. Less-Common Met.* 53 (1977) 193.

[27] A.P. Gonçalves, J.C. Waerenborgh, G. Bonfait, A. Amaro, M.M. Godinho, M. Almeida, J.C. Spirlet, *J. Alloys Compd.* 204 (1994) 59.

[28] S.K. Dhar, K.V. Shah, P. Bonville, P. Manfrinetti, F. Wrubl, *Sol. State Commun*. 147 (2008) 217

[29] G. Nolze, W. Krauss, PowderCell 2.3 Program, BAM Berlin (2000).

[30] http://www.ill.eu/sites/fullprof/.

[31] Bruker-AXS, In: Collect, Denzo, Scalepack, Sortav. Kappa CCD Program Package, Delft, The Netherlands, 1998.

[32] Z. Otwinowski, W. Minor, *Processing of X-ray diffraction data collected in oscillation mode, Methods in enzymology*, in: C.W. Carter Jr., R.M. Sweet (Eds.), Macromolecular Crystallography, part A, Vol. 276, Academic Press, 1997, pp. 307–326.

[33] R.H. Blessing, *Acta Crystallogr*. A 51 (1995) 33.

[34] A. Altomare, M.C. Burla, M. Camalli, G.L. Cascarano, C. Giacovazzo, A. Guagliardi, A.G.G. Moliterni, G. Polidori, R.J. Spagna, *J. Appl. Crystallogr*. 32 (1999) 115.

[35] G.M. Sheldrick, SHELXS-97 and SHELXL-97. Programs for Structure Solution and Refinement, University of Göttingen, Germany, 1997.

[36] E. Parthé , K. Cenzual, R. Gladyshevskii, *J. Alloys Compd*. 197 (1993) 291.

[37] T. Le Bihan, H. Noel, P. Rogl, *J. Alloys Compd*. 240 (1996) 128.

[38] D. Berthebaud, O. Tougait, M. Potel, E.B. Lopes, A.P. Gonçalves, H. Noel, *J. Solid State Chem*. 180 (2007) 2926.

[39] C. Krellner, S. Lausberg, A. Steppke, M. Brando, L. Pedrero, H. Pfau, S. Tence, H. Rosner, F. Steglich, C. Geibel, *New J. Phys.* 13 (2011)103014.

Figure captions:

Figure 1 - Prepared compositions of U–Fe–Ge alloys (△, ▲: three-phase samples; □, ■ : two-phase samples; ○, ●: single-phase samples). The full black symbols correspond to selected samples for which compositions and chemical analysis are given in Table 2.

Figure 2 - Isothermal section at 900ºC of the U-Fe-Ge system: $UFe_{2-x}Ge_x$ (*A*), $U_2Fe_{17-x}Ge_x$ (*B*), U_2Fe_3Ge (*C*), $U_6Fe_{16}Ge_7$ (*D*), UFe_4Ge_2 (*E*), $U_6Fe_{22}Ge_{13}$ (*F*), UFeGe (*G*), $U_3Fe_4Ge_4$ (*H*), UFe_2Ge_2 (*I*), $UFe_{6+x}Ge_{6-x}$ (*J*), $U_{34}Fe_{3.32}Ge_{33}$ (*K*), $UFe_{1-x}Ge_2$ (*L*), $U_3Fe_2Ge_7$ (*M*), and $U_9Fe_7Ge_{24}$ (*N*), (thick black lines: solid solutions; dash tie-lines: extrapolations; grey area: liquid region; thick dash grey line: liquid line).

Figure 3 - Scanning electron micrograph (backscattered mode) of a sample with nominal composition 28U:54Fe:18Ge annealed at 900°C, showing the phases (*a*) U_2Fe_3Ge, (*b*) $U_6Fe_{16}Ge_7$, and (*c*) $U_2Fe_{15}Ge_2$, according to the EDS results.

Figure 4 – Experimental powder X-ray diffraction pattern for the annealed sample of $U_3Fe_4Ge_4$ (red open symbols) with the Rietveld calculated pattern (black line) and the difference profile (bottom blue line). The calculated Bragg positions for $U_3Fe_4Ge_4$ are marked by the green vertical bars. Remaining peaks belong to UFe_2Ge_2 present in the sample.

Figure 5 – Experimental powder X-ray diffraction pattern for the annealed sample of $U_{34}Fe_{3.32}Ge_{33}$ (red open symbols) with the Rietveld calculated pattern (black line) and the difference profile (bottom blue line). The calculated Bragg positions for $U_{34}Fe_{3.32}Ge_{33}$ are marked by the green vertical bars.

Figure 6 –Scanning electron micrograph (backscattered mode) of a sample with nominal composition U:0.75Fe:2Ge annealed at 900ºC for three days. The EDS results show atomic compositions compatible with (a) UFe_2Ge_2, (b) $UFe_{0.4}Ge_2$ and (c) $U_3Fe_2Ge_7$.

Figure 7 –Scanning electron micrograph (backscattered mode) of a sample with nominal composition U:Fe:3Ge annealed at 900ºC for three days. The phases present are (a) $U_9Fe_7Ge_{24}$, (b) UGe_3 and (c) UFe_6Ge_6.

Figure 8 - X-ray diffraction pattern of a sample with composition 12U:60Fe:28Ge annealed at 900°C (red open symbols) with the Rietveld fitting (black line) and the difference profile (bottom blue line). It shows the calculated Bragg positions for UFe_4Ge_2 (green vertical bars) as the main phase (71%). The remaining peaks were indexed as $U_6Fe_{22}Ge_{13}$, estimated to be 29% of the sample.

Figure 9 – View of the tetragonal crystal structure of UFe_4Ge_2 along *c* with the U atoms located in the channels between chains of edge-connected Fe tetrahedra. The coordination polyhedron for U is shown in the upper right corner of the unit cell (light blue).

Figure 10 – (*a*) Unit cell of $U_6Fe_{22}Ge_{13}$ and (*b*) coordination polyhedra for the U atoms in different Wyckoff sites.

Figure 11 –Scanning electron microscope micrograph (backscattered mode) of an annealed sample with nominal composition 5.3U:22.2Fe:13.5Ge, showing equilibrium between the phases (a) UFe_2Ge_2, (b) $U_6Fe_{22}Ge_{13}$, and the binary (c) Fe_3Ge.

Figure 12 – Unit cell of $UFe_{0.4}Ge_2$ and coordination polyhedron for the U atoms.

FIGURES:

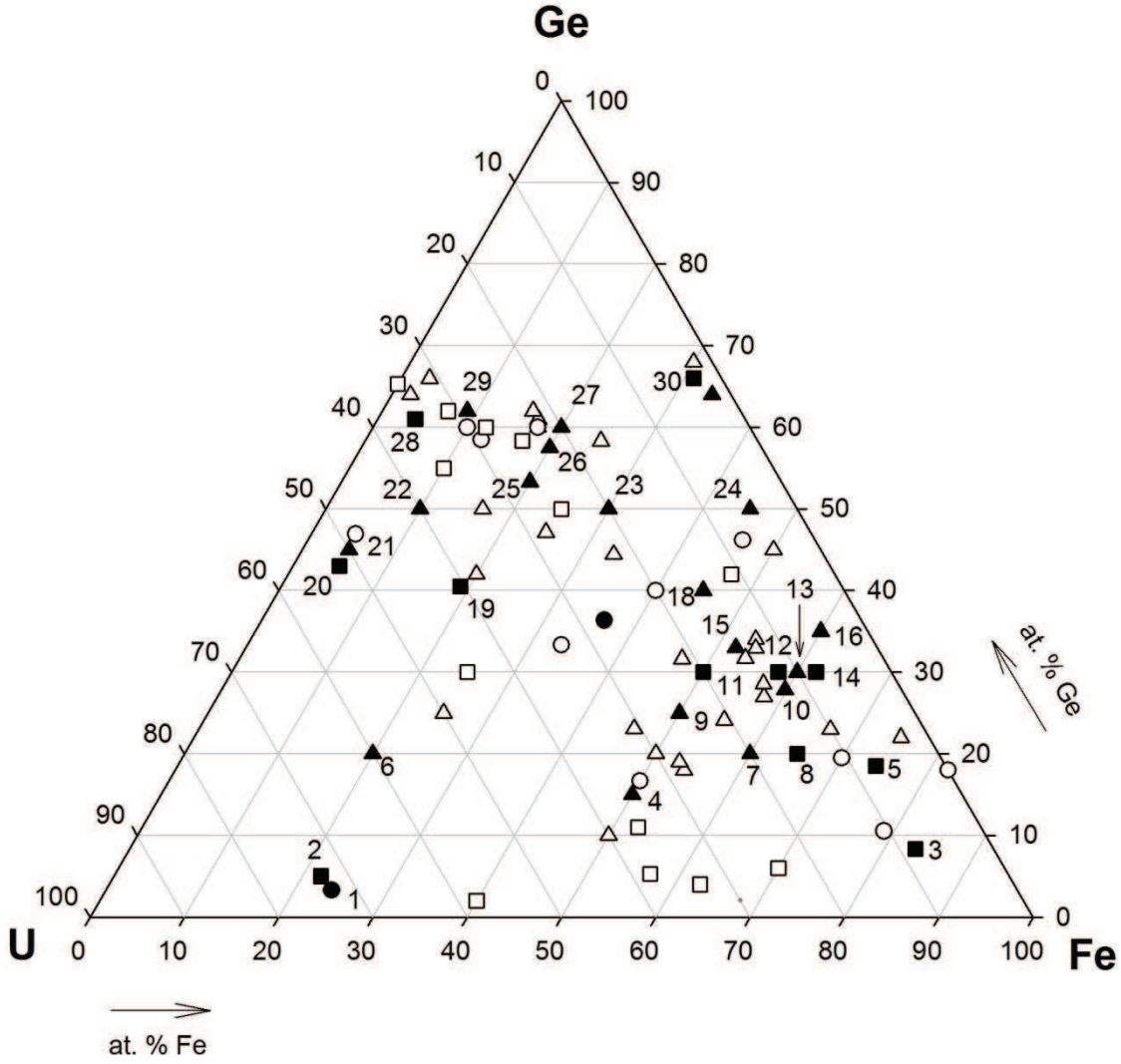

Figure 1

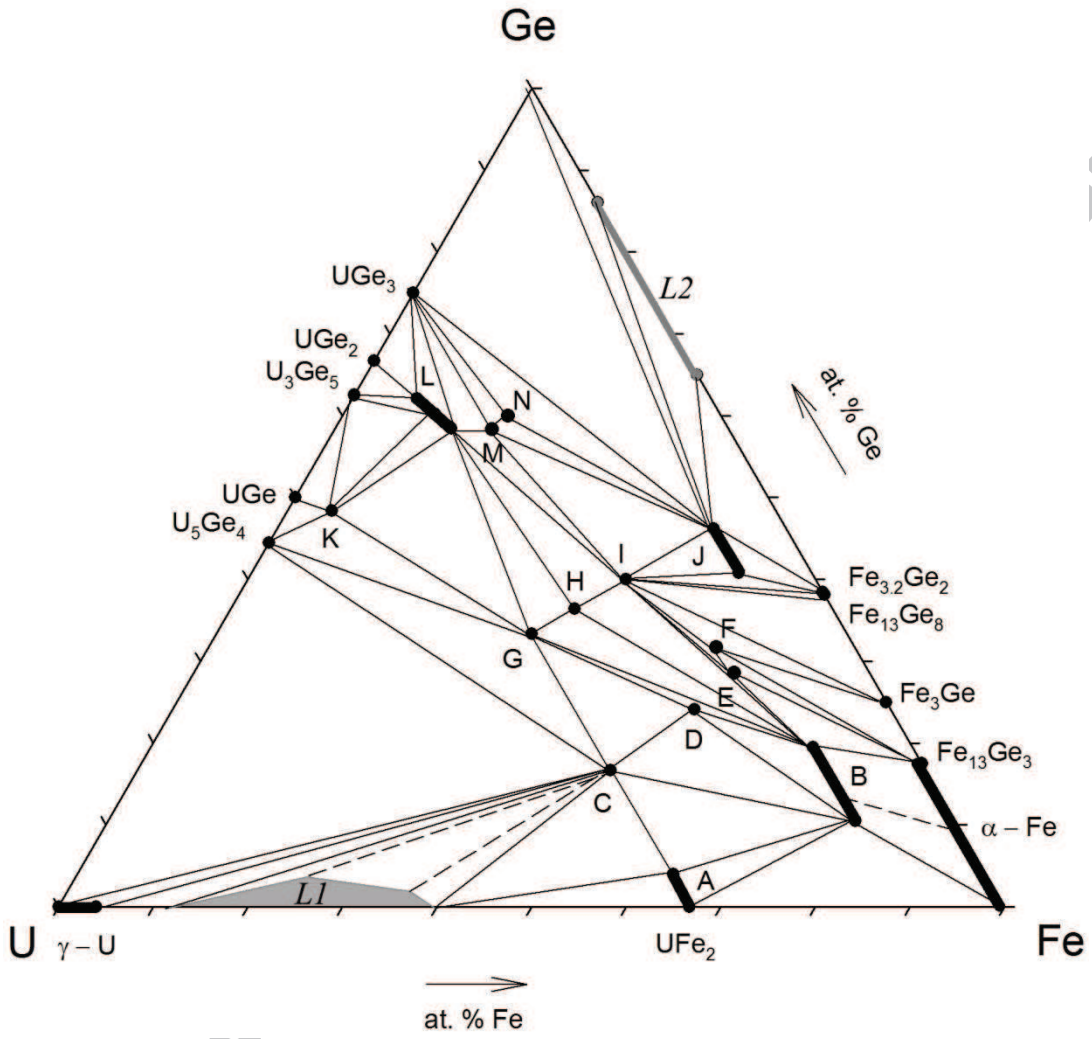

Figure 2

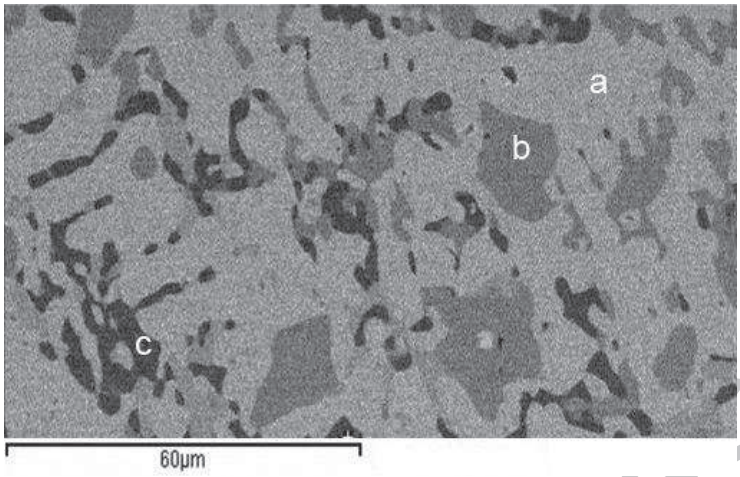

Figure 3

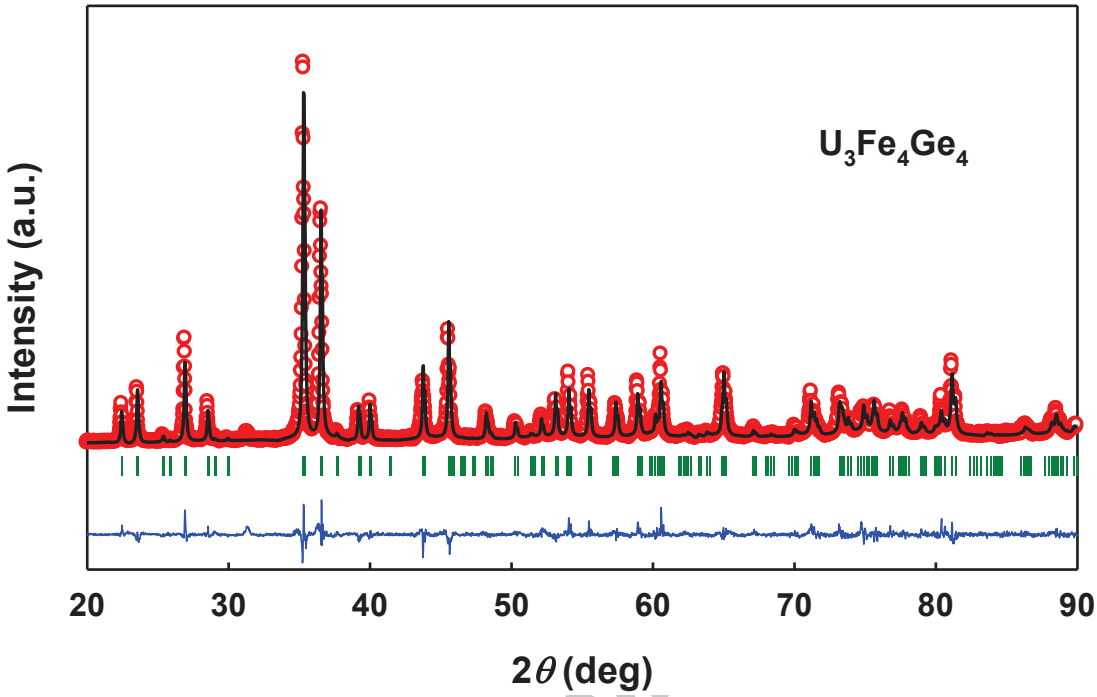

Figure 4

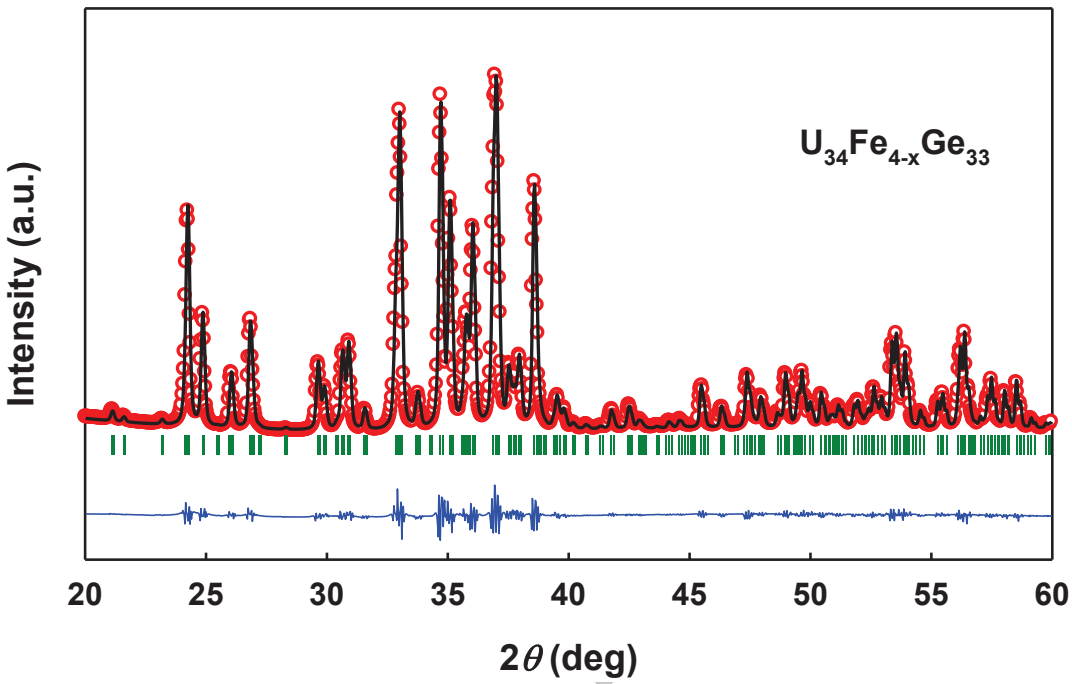

Figure 5

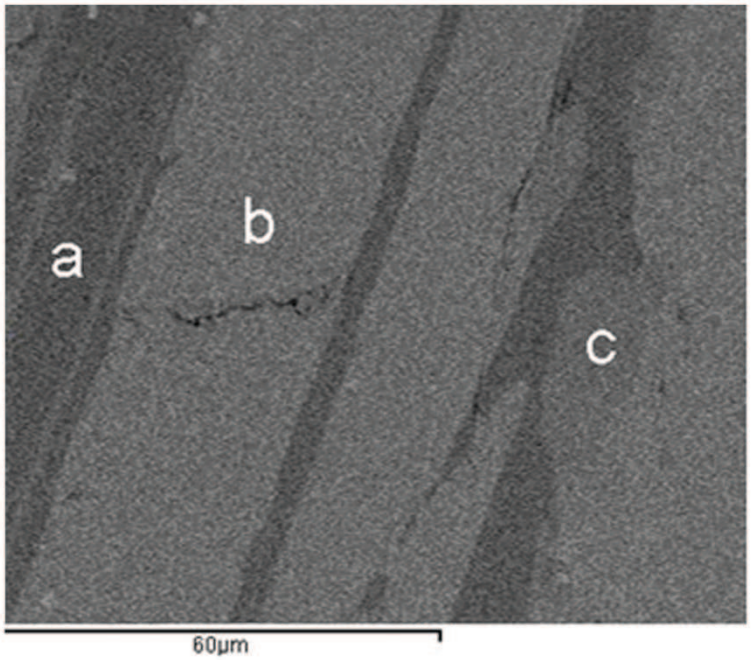

Figure 6

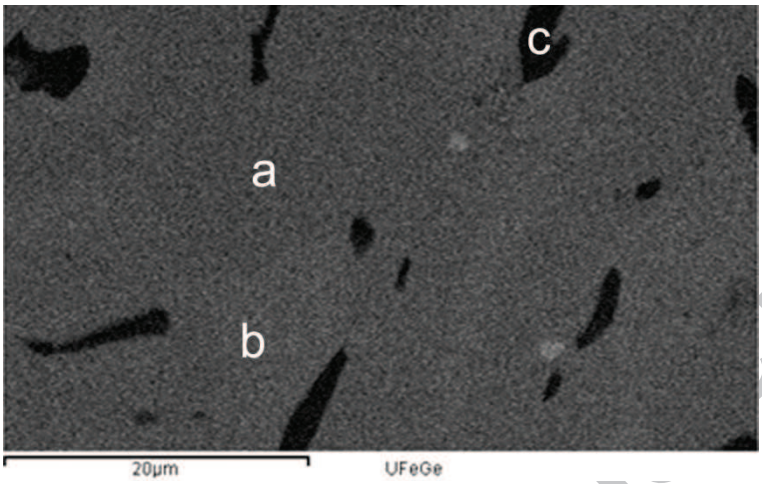

Figure 7

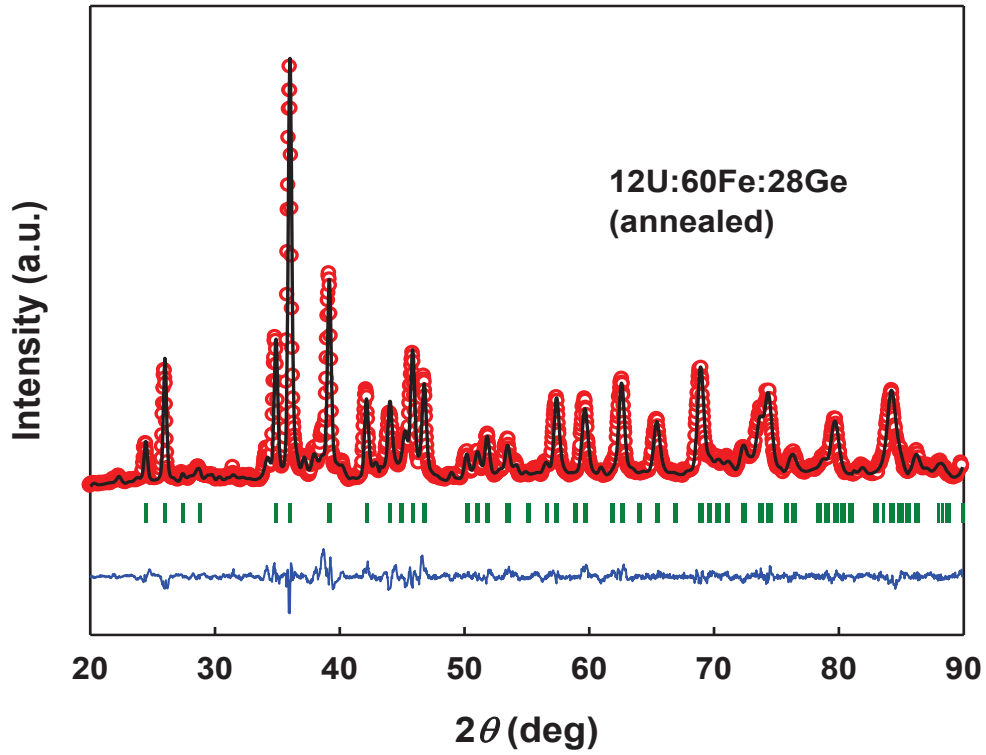

Figure 8

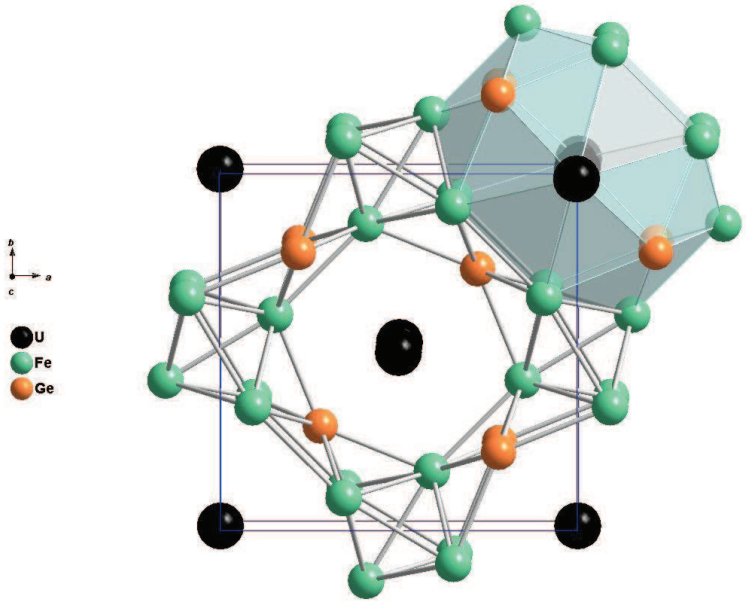

Figure 9

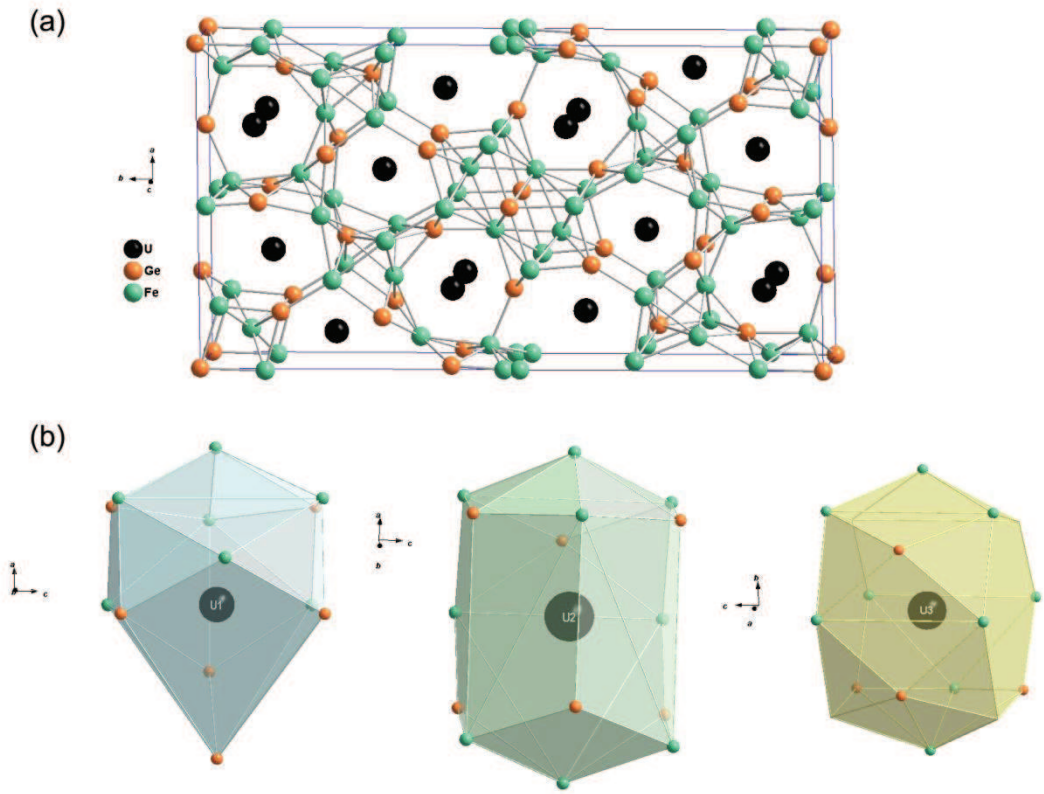

Figure 10

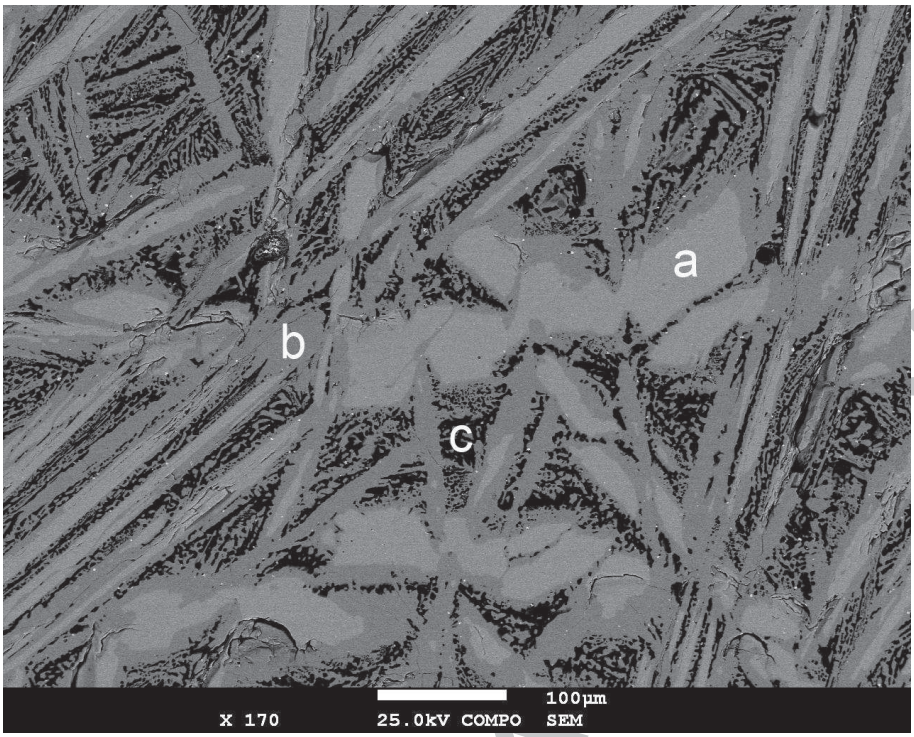

Figure 11

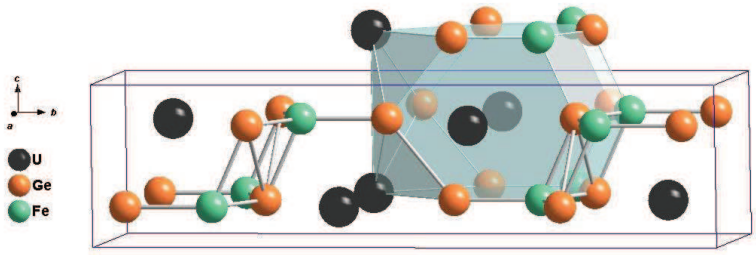

Figure 12

Tables

Table 1 – Reported crystallographic data for unary, binary, and ternary solid phases in the U-Fe-Ge system.

Phase	Transformation temperature (°C)	Structure type	Space group	Lattice parameters (Å)			Ref.
				a	*b*	*c*	
U (α)	662, *t*	U	*Cmcm*	2.8537	5.870	4.955	[*d*]
U (β)	772, *t*	CrFe	$P4_2/mnm$	10.7589	--	5.653	[*e*]
U (γ)	1132, *m*	W	$Im\bar{3}m$	3.5335	--	--	[*e*]
Fe (α)	910, *t*	W	$Im\bar{3}m$	2.8665	--	--	[*f*]
Fe (γ)	1390, *t*	Cu	$Fm\bar{3}m$	3.6599	--	--	[*f*]
Fe (δ)	1535, *m*	W	$Im\bar{3}m$	2.9315	--	--	[*f*]
Ge	938, *m*	C diamond	$Fd\bar{3}m$	5.621	--	--	[22, *g*]
UFe_2	1235, *m*	$MgCu_2$	$Fd\bar{3}m$	7.055	--	--	[21]
U_6Fe	805, *p*	U_6Mn	*I4/mcm*	10.3022	--	5.239	[21]
UGe_3	1475, *m*	$AuCu_3$	$Pm\bar{3}m$	4.196	--	--	[22, *h*]
UGe_2	1450, *m*	$ZrGa_2$	*Cmmm*	4.036	14.928	4.116	[22, *i*]
UGe_{2-x} ($0.3<x<0.45$)	--	$ThSi_2$	$I4_1/amd$	4.035 (x=0.35)	--	13.903	[23]
U_3Ge_5	--	AlB_2	*P6/mmm*	3.954	--	4.125	[*j*]
UGe	--	ThIn	*Pbcm*	9.827	8.932	5.841	[*k*]
U_5Ge_4	1670, *m*	Ti_5Ga_4	$P6_3/mcm$	8.744	--	5.863	[22, *l*]
$Fe_{13}Ge_3$	--	$Fe_{13}Ge_3$	$Pm\bar{3}m$	5.763	--	--	[*n*]
$Fe_{3.2}Ge_2$	1130, *m*	$Fe_{3.2}Ge_2$	$P6_3/mcm$	3.998	--	5.010	[22]
$Fe_{13}Ge_8$	928, *p*	$Fe_{13}Ge_8$	$P6_3/mcm$	7.976	--	4.993	[22]
Fe_3Ge	1122, *p*	Ni_3Sn	*P6/mmc*	5.162	--	4.207	[22]
$U_2Fe_{17-x}Ge_x$ ($2<x<3$)	--	Th2Ni17	$P6_3/mmc$	8.435(3) (x = 3)	--	8.370(4)	[24]
UFeGe	--	TiNiSi T> 500K	*Pnma*	6.828(2)	4.259(1)	7.286(2)	[25]
	--	UFeGe T<500K	$P2_1/m$	6.986(1)	4.308(1)	6.992(1) β = 93.71°	[25]
UFe_2Ge_2	--	$ThCr_2Si_2$	*I4/mmm*	4.016(2)	--	9.961(7)	[26]
UFe_6Ge_6	--	YCo_6Ge_6	*P6/mmm*	5.126(8)	--	4.050(5)	[27]
U_2Fe_3Ge	--	$MgZn_2$	$P6_3/mmc$	5.187(3)	--	7.850(5)	[14,28]
$U_3Fe_4Ge_4$	--	$Gd_3Cu_4Ge_4$	*Immm*	4.090(1)	6.639(1)	13.702(1)	[18]
$U_{34}Fe_{4-x}Ge_{33}$	--	$U_{34}Fe_{4-x}Ge_{33}$	*I4/mmm*	10.873(5) (x = 0.68)	--	25.274(3)	[19]

$U_3Fe_2Ge_7$	--	$La_3Co_2Sn_7$	*Cmmm*	4.167(7)	24.982(2)	4.156(3)	[20]
$U_9Fe_7Ge_{24}$	--	$U_9Fe_7Ge_{24}$	*I4/mmm*	12.379(2)	--	18.288(3)	[16]

t- solid state transition; *m*- melting point; *p*- peritectic reaction

[*d*] C.S. Barrett, M.H. Mueller, R.L. Hitterman, *Phys. Rev*. *B* 129 (1963) 625.

[*e*] A.C. Lawson, C.E. Olsen, J.W. Richardson Jr, M.H. Mueller, G.H. Lander, *Acta Crystallogr. B* 44 (1988) 89.

[*f*] R. Kohlhaas, P. Dünner, N. Schmitz-Pranghe*, Z. Angew. Phys.* 23 (1967) 245.

[*g*] A.V. Morozkin, Y.D. Seropegin, *J. Alloys Compd.* 365 (2004) 168.

[*h*] L.H Brixner, *J. Inorg. Nuclear Chem.* 25 (1963) 783.

[*i*] P. Boulet, A. Daoudi, M. Potel, H. Noel, G.M.Gross, G. Andre, F. Bouree, *J. Alloys Compd.* 247 (1997) 104.

[*j*] P. Boulet, M. Potel, G. Andre, P. Rogl, H. Noel, *J. Alloys Compd*. 283 (1999) 41.

[*k*] P. Boulet, A. Daoudi, M. Potel, H. Noel, *J. Solid State Chem.* 129 (1997) 113.

[*l*] P. Boulet, M. Potel, J.C. Levet, H. Noel, *J. Alloys Compd*. 262 (1997) 229.

[*n*] P. Lecocq, A. Michel, *Bull. Soc. Chim.* (1962) 1412.

Table 2 – EDS data on selected U-Fe-Ge samples marked in Fig. 1, after annealing at 900ºC. All compositions are given in at.%.

Sample	Nominal composition			Phases	EDS composition		
	U	Fe	Ge		U	Fe	Ge
1	72.7	24	3.3	*L*1	83.49	14.07	2.45
2	73	22	5	*L*1	84.69	13.88	1.63
				U_2Fe_3Ge	*		
3	8.3	83.3	8.3	$U_2Fe_{17-x}Ge_x$	11.77	78.09	10.14
				α-Fe	0.14	98.55	1.31
4	35	50	15	U_2Fe_3Ge	35.76	47.57	16.67
				$UFe_{2-x}Ge_x$	33.86	58.58	6.59
				*L*1	*		
5	7.4	74	18.5	$U_2Fe_{17-x}Ge_x$	11.67	67.43	20.90
				α-Fe	0.34	82.42	17.24
6	60	20	20	U_5Ge_4	54.93	0.22	44.86
				U_2Fe_3Ge	33.83	49.30	16.86
				γ-U	99.08	0.86	0.07
7	20	60	20	$U_6Fe_{16}Ge_7$	19.61	56.48	24.31
				$UFe_{17-x}Ge_x$	10.23	68.53	21.24
				U_2Fe_3Ge	33.83	49.30	16.86
8	15	65	20	$UFe_{17-x}Ge_x$	10.63	72.17	17.20
				$U_6Fe_{16}Ge_7$	20.37	56.36	23.27
9	25	50	25	U_2Fe_3Ge	32.02	51.17	16.81
				$U_6Fe_{16}Ge_7$	20.31	55.97	23.72
				UFeGe	33.00	32.42	34.58
10	12.4	59.8	27.8	UFe_4Ge_2	11.70	62.39	25.91
				$U_6Fe_{22}Ge_{13}$	14.41	52.25	33.35
				α-Fe	*		
11	20	50	30	$U_3Fe_4Ge_4$	28.32	34.52	37.17
				$U_2Fe_{17-x}Ge_x$	10.30	68.74	20.96
12	12	58	30	$U_6Fe_{22}Ge_{13}$	14.86	53.83	31.31
				α-Fe	0.18	82.06	17.76
13	10	60	30	$U_6Fe_{22}Ge_{13}$	14.83	52.38	32.78
				Fe_3Ge	0.60	74.24	25.16
				UFe_2Ge_2	18.76	39.58	41.66
14	8	62	30	UFe_2Ge_2	19.61	39.85	40.54
				Fe_3Ge	0.33	74.36	25.47
15	15	52	33	$U_6Fe_{22}Ge_{13}$	13.77	51.67	34.56
				UFe_2Ge_2	19.33	40.08	40.59
				Fe_3Ge	*		
16	5	60	35	$Fe_{13}Ge_8$	0.29	63.95	35.78
				Fe_3Ge	0.35	75.20	24.42
				UFe_2Ge_2	18.20	41.73	40.07
17	27.3	36.3	36.3	$U_3Fe_4Ge_4$	29.01	34.96	36.04
18	15	45	40	UFe_2Ge_2	21.12	38.43	40.45
				$UFe_{6+x}Ge_{6-x}$	8.71	46.70	44.59
				$Fe_{3.2}Ge_2$	0.26	62.77	36.98
19	40.5	18.9	40.5	$U_{34}Fe_{4-x}Ge_{33}$	49.29	3.62	47.09
				UFeGe	34.00	32.68	33.32
20	52	5	43	U_5Ge_4	54.93	0.22	44.86
				UFeGe	33.20	32.90	33.90
21	50	5	45	$U_{34}Fe_{4-x}Ge_{33}$	50.53	3.88	45.59

				U_5Ge_4	55.63	0.17	44.21
				UFeGe	34.10	32.12	33.16
22	40	10	50	$U_{34}Fe_{4-x}Ge_{33}$	49.15	4.42	46.42
				$UFe_{1-x}Ge_2$	27.57	16.89	55.53
				UFeGe	33.31	32.82	33.87
23	20	30	50	$U_3Fe_2Ge_7$	35.76	47.57	16.67
				$UFe_{6+x}Ge_{6-x}$	33.86	58.58	6.59
				UFe_2Ge_2	57.96	0.62	41.41
24	05	45	50	$UFe_{6+x}Ge_{6-x}$	7.77	45.64	46.59
				*L*2	0.00	34.26	65.83
				$Fe_{3.2}Ge_2$	0.06	63.26	36.68
25	27	20	53	$UFe_{1-x}Ge_2$	27.91	16.90	55.30
				$U_3Fe_2Ge_7$	26.03	15.15	58.82
				UFe_2Ge_2	20.34	39.55	41.11
26	22.5	20	57.5	$U_9Fe_7Ge_{24}$	21.92	17.49	60.59
				$U_3Fe_2Ge_7$	22.63	17.65	59.72
				$UFe_{6+x}Ge_{6-x}$	8.87	44.67	46.45
27	20	20	60	$U_9Fe_7Ge_{24}$	21.92	17.49	60.59
				UGe_3	24.48	1.26	74.25
				$UFe_{6+x}Ge_{6-x}$	7.79	46.06	46.14
28	35	4	61	$UFe_{1-x}Ge_2$	28.65	8.81	62.54
				U_3Ge_5	35.38	0.47	64.15
29	29	9	62	$UFe_{1-x}Ge_2$	29.37	14.57	56.06
				UGe_3	27.34	0.93	71.73
30	3	31	66	*L*2	0.00	34.26	65.83
				$UFe_{6+x}Ge_{6-x}$	8.29	47.47	44.14

* not quantified

Table 3 – Crystallographic data for the ternary U-Fe-Ge compounds and solid solutions stable in the U-Fe-Ge isothermal section at 900ºC.

Phase	Structure type	Space group	Lattice parameters (Å)		
			a	*b*	*c*
(*A*) $UFe_{2-x}Ge_x$ (x<0.15)	$MgCu_2$	*Fd*$\bar{3}$*m*	7.097(1) (x = 0.15)	--	--
(*B*) $U_2Fe_{17-x}Ge_x$ (2<x<3.7)	Th_2Ni_{17}	*P*6$_3$/*mmc*	8.480(1) (x = 3.7)	--	8.367(6)
(*C*) U_2Fe_3Ge	Mg_2Cu_3Si	*P*6$_3$/*mmc*	5.187(3)	--	7.850(5)
(*D*) $U_6Fe_{16}Ge_7$	$Mg_6Cu_{16}Si_7$	*Fm*$\bar{3}$*m*	11.923(6)	--	--
(*E*) UFe_4Ge_2	$ZrFe_4Si_2$	*P*4$_2$/*mnm*	7.283(1)	--	3.851(1)
(*F*) $U_6Fe_{22}Ge_{13}$	$U_6Fe_{22}Ge_{13}$	*Pbam*	12.674(5)	24.196(5)	4.005(5)
(*G*) UFeGe	TiNiSi T> 500K	*Pnma*	6.772(1)	4.200(1)	7.266(2)
	UFeGe T<500K	*P*2$_1$/*m*	6.980(1)	4.309(1)	6.996(7) β = 93.72º
(*H*) $U_3Fe_4Ge_4$	$Gd_3Cu_4Ge_4$	*Immm*	4.086(5)	6.640(5)	13.686(5)
(*I*) UFe_2Ge_2	$ThCr_2Si_2$	*I*4/*mmm*	4.016(5)	--	9.960(6)
(*J*) $UFe_{6+x}Ge_{6-x}$ (x<0.8)	YCo_6Ge_6	*P*6/*mmm*	5.125(2) (x = 0)	--	4.048(6)
(K) $U_{34}Fe_{3.32}Ge_{33}$	$U_{34}Fe_{3.32}Ge_{33}$	*I*4/*mmm*	10.875(5)	--	25.250(5)
(*L*) $UFe_{1-x}Ge_2$ (0.58<x<0.78)	$CeNiSi_2$	*Cmcm*	4.083(5) (x = 0.6)	15.805(5)	4.030(5)
(*M*) $U_3Fe_2Ge_7$	$La_3Co_2Sn_7$	*Cmmm*	4.153(1)	24.927(1)	4.155(1)
(*N*) $U_9Fe_7Ge_{24}$	$U_9Fe_7Ge_{24}$	*I*4/*mmm*	12.379(2)	--	18.288(3)

Table 4 – Parameters for X-ray powder diffraction data collection and structural refinements for the UFe_4Ge_2 compound.

Chemical formula	**UFe_4Ge_2**
Space group	$P4_2/mnm$ (No. 136)
Cell parameters (Å)	
a	7.2739 (4)
c	3.8838 (3)
Cell volume (Å^3)	205.5(2)
Wavelengths (Å)	1.54060, 1.54443 (Cu K_α)
Data range (2θ deg)	20-90
Counting step (2θ deg)	0.030
Number of points	2335
Counting time per step (s)	10
Number of reflections	141/2
Zero point (2θ deg)	0.1034(27)
η (pseudo–Voigt)	0.363(33)
Halfwidth parameters	
U	0.6754(66)
V	-0.1941(58)
W	0.0891(13)
Rietveld reliability factors (%)	
R_P	6.64
R_{WP}	8.81
χ^2	2.17
R_B	3.79
R_F	2.22

Table 5 – Atomic coordinates and isotropic displacement parameters (U_{eq}) and their estimated standard deviations for UFe_4Ge_2.

Atom	**Site**	***x***	***y***	***z***	U_{eq} (Å^2)[a]
U	2*b*	0	0	1/2	0.0449(5)
Fe	8*i*	0.6494(6)	0.9065(5)	0	0.0422(9)
Ge	4*g*	0.7841(4)	0.2159(4)	0	0.0153(12)

[a] U_{eq} is defined as one-third of the trace of the orthogonalized U_{ij} tensor.

Table 6 – Selected interatomic distances for UFe_4Ge_2.

Atom pair		Distance (Å)	Atom pair		Distance (Å)	Atom pair		Distance (Å)
U	4Ge	2.882(1)	Fe	2Ge	2.411(7)	Ge	1Fe	2.191(7)
	2Ge	2.974(1)		1Ge	2.452(5)		2Ge	2.618(7)
	8Fe	3.173(2)		1Fe	2.603(3)		4U	2.981(8)
	4Fe	3.245(3)		1Fe	2.623(6)		2U	3.215(8)
	2Ge	3.215(8)		4Fe	2.663(3)			
	2U	3.851(0)		1U	3.173(2)			
				2U	3.245(3)			

Table 7 – Selected single-crystal X-ray diffraction data collection and refinement parameters for $U_6Fe_{22}Ge_{13}$.

Chemical formula	**$U_6Fe_{22}Ge_{13}$**
Formula weight (g mol^{-1})	900
Crystal system	Orthorhombic
Space group	*Pbam* (No. 55)
Lattice parameters (Å)	a=12.6740(5), b=24.1960(5) c=4.0050(5)
Cell volume (Å^3)	1228.17(1)
Formula per unit cell (Z), Calculated density (g cm^{-3})	8, 9.74
Radiation, Wavelenght (Å)	Mo Kα, 0.71073
θ range (º)	3-35
Data set	-20≤h≤20, -36≤k ≤39, -6≤l≤6
Collected / Unique reflections / R_{int}	20892/3015/0.085
Refined parameters	126
Final agreement factors (I>2σ(I)) R, ωR_2 [b]	0.034, 0.088
Goodness of the fit	1.032
Extinction coefficient	0.0004
Highest/lowest peak of electron density (e-/Å^3)	4.706/-5.915

[b] $R(F) = \Sigma\left|\left|F_o\right| - \left|F_c\right|\right| / \left|F_c\right|$, $\omega R_2 = [\Sigma\omega(F_o^2 - F_c^2)^2/\omega F_o^4]^{1/4}$, where $\omega^{-1} = [\sigma^2(F_o^2) + 7.27P]$, with σ is the estimated standard deviation and $P = [\max(F_o^2, 0) + 2(F_c^2)]/3$ is the number of parameters.

Table 8 – Atomic coordinates and isotropic displacement parameters (U_{eq}) and their estimated standard deviations for $U_6Fe_{22}Ge_{13}$.

Atom	Site	*x*	*y*	*z*	U_{eq} (Å^2)
U1	4*g*	0.2497(1)	0.0927(6)	0	0.0115(7)
U2	4*h*	0.1578(3)	0.3898(8)	1/2	0.0103(1)
U3	4*h*	0.4091(4)	0.2902(8)	1/2	0.0131 (8)
Fe1	4*g*	0.2274(1)	0.2860(6)	0	0.0108(1)
Fe2	4*g*	0.1003(1)	0.4875(1)	0	0.0115(3)
Fe3	4*g*	0.1057(2)	0.2003(6)	0	0.0162(6)
Fe4	4*h*	0.2379(6)	0.1967(7)	1/2	0.0121(8)
Fe5	4*h*	0.4241(9)	0.1554(2)	1/2	0.0139(2)
Fe6	4*h*	0.4498(5)	0.0447(2)	1/2	0.0127(1)
Fe7	4*h*	0.4012(1)	0.4270(7)	1/2	0.0110(1)
Fe8	4*g*	0.0057(1)	0.1042(5)	0	0.0112(1)
Fe9	4*g*	0.0277(6)	0.3029(1)	0	0.0116(8)
Fe10	4*h*	0.0921(5)	0.0331(5)	1/2	0.0119(5)
Fe11	4*g*	0.3083(8)	0.4685(1)	0	0.0134(3)
Ge1	4*h*	0.0935(1)	0.1324(6)	1/2	0.0113(0)
Ge2	4*h*	0.2745(5)	0.0045(1)	1/2	0.0113(8)
Ge3	4*h*	0.01150(0)	0.2726(3)	1/2	0.0166(6)
Ge4	4*g*	0.3248(3)	0.3696(7)	0	0.0111(9)
Ge5	2*a*	0	0	0	0.0123(5)
Ge6	4*g*	0.4879(1)	0.0967(1)	0	0.0110(6)
Ge7	4*g*	0.3401(5)	0.2065(6)	0	0.0121(2)

Table 9 – Selected interatomic distances for $U_6Fe_{22}Ge_{13}$.

Atom pair		Distance (Å)	Atom pair		Distance (Å)	Atom pair		Distance (Å)
U1	2Ge2	2.942(8)	U2	1Ge3	2.888(3)	U3	2Ge4	2.974(8)
	2Ge1	2.975(8)		1Ge2	2.902(4)		2Ge7	2.979(8)
	1Ge7	2.983(5)		2Ge4	2.955(8)		1Ge3	3.019(7)
	1Ge6	3.021(2)		2Ge6	2.959(8)		2Fe1	3.054(8)
	1Fe11	3.092(4)		1Fe6	3.075(7)		1Ge1	3.054(8)
	1Fe8	3.104(2)		1Fe5	3.157(5)		1Fe4	3.134(8)
	2Fe10	3.174(9)		2Fe2	3.181(8)		2Fe3	3.205(8)
	1Fe2	3.176(8)		1Fe7	3.212(5)		1Fe5	3.266(2)
	1Fe3	3.179(8)		2Fe1	3.334(9)		1Fe7	3.312(2)
	2Fe4	3.219(8)		2Fe9	3.340(1)		2Fe9	3.367(1)
	2Fe5	3.347(1)		2Fe11	3.356(1)		2Fe8	3.472(1)
	2Fe6	3.434(9)						
Ge1	2Fe8	2.390(6)	Ge2	1Fe10	2.413(4)	Ge3	2Fe9	2.402(6)
	1Fe4	2.402(6)		2Fe11	2.423(6)		1Fe4	2.411(6)
	1Fe10	2.402(2)		1Fe6	2.425(5)		2Fe1	2.478(6)
	2Fe3	2.595(7)		2Fe2	2.587(7)		2Fe3	2.663(7)
	1Fe7	2.828(6)		1U2	2.902(4)		1U2	2.888(3)
	2U1	2.975(8)		1Fe7	2.913(7)		1Fe5	2.980(7)
	1U3	2.997(7)		4U1	2.942(8)		1U3	3.019(7)
							1Ge1	3.406(2)
Ge4	1Fe1	2.370(6)	Ge5	4Fe10	2.452(6)	Ge6	2Fe6	2.414(6)
	1Fe8	2.380(4)		2Fe8	2.522(1)		1Fe2	2.485(6)
	1Fe11	2.404(2)		2Fe11	2.547(4)		1Fe9	2.482(3)
	2Fe7	2.622(7)		4Fe7	2.950(6)		2Fe5	2.584(7)
	2U2	2.955(8)					1Fe2	2.869(5)
	2U3	2.974(8)					2U2	2.959(8)
							1U1	3.021(2)
							1Ge7	3.249(8)
Ge7	1Fe9	2.388(2)	Fe1	1Ge4	2.370(6)	Fe2	1Ge6	2.485(6)
	1Fe1	2.396(6)		1Ge7	2.396(6)		2Fe6	2.516(7)
	2Fe4	2.397(6)		2Ge3	2.478(6)		2Ge2	2.587(7)
	2Fe5	2.583(7)		1Fe9	2.563(3)		1Fe2	2.613(4)
	1Fe3	2.975(2)		1Fe3	2.584(6)		1Fe11	2.675(3)
	1U1	2.983(5)		2Fe4	2.949(8)		1Ge6	2.869(5)
	1Ge6	3.249(8)		2U3	3.054(6)		2Fe6	2.873(8)
	2U2	3.351(9)		2U2	3.334(9)		1U1	3.176(8)
							2U2	3.181(8)

Fe3	1Fe1	2.584(6)	Fe4	2Ge7	2.397(6)	Fe5	1Fe4	2.563(5)
	2Ge1	2.595(7)		1Ge1	2.402(6)		2Ge7	2.583(7)
	2Fe4	2.613(7)		1Ge3	2.411(6)		2Ge6	2.584(7)
	1Fe8	2.647(6)		1Fe5	2.563(5)		2Fe9	2.599(7)
	2Ge3	2.663(7)		2Fe3	2.613(7)		1Fe6	2.698(3)
	1Fe9	2.673(5)		2Fe1	2.949(8)		1Ge3	2.980(7)
	1Ge7	2.975(2)		1U3	3.134(8)		1U2	3.157(5)
	1U1	3.179(8)		2U1	3.219(8)		1U3	3.266(2)
	2U3	3.205(8)					2U1	3.347(1)
Fe6	2Ge6	2.414(6)	Fe7	2Fe8	2.517(7)	Fe8	1Ge4	2.380(4)
	1Ge2	2.425(5)		2Fe11	2.532(7)		2Ge1	2.390(6)
	1Fe6	2.508(6)		1Fe10	2.569(2)		2Fe7	2.517(7)
	2Fe2	2.516(7)		1Fe10	2.607(5)		1Ge5	2.522(1)
	1Fe5	2.698(3)		2Ge4	2.622(7)		1Fe3	2.647(6)
	2Fe2	2.873(8)		1Ge1	2.828(6)		2Fe10	2.858(8)
	1U2	3.075(7)		1Ge2	2.913(7)		1Fe11	3.060(7)
	2U1	3.434(9)		2Ge5	2.950(8)		1U1	3.104(2)
				1U3	3.312(2)		2U3	3.472(1)
				1U2	3.312(5)			
Fe9	1Ge7	2.388(2)	Fe10	Ge1	2.402(2)	Fe11	1Ge4	2.404(2)
	2Ge3	2.402(6)		1Ge2	2.413(4)		2Ge2	2.423(6)
	1Ge6	2.482(3)		2Ge5	2.452(6)		2Fe7	2.532(7)
	1Fe1	2.563(3)		1Fe7	2.569(2)		1Ge5	2.547(4)
	2Fe5	2.599(7)		1Fe7	2.607(5)		1Fe2	2.675(3)
	1Fe3	2.673(5)		1Fe10	2.831(7)		2Fe10	2.836(8)
	2U2	3.34(1)		2Fe11	2.836(8)		1Fe8	3.060(7)
	2U3	3.367(1)		2Fe8	2.858(8)		2U1	3.092(4)
				2U1	3.174(9)		2U2	3.356(1)

Table 10 – Parameters for X-ray powder diffraction data collection and structural refinements for the compound $UFe_{0.4}Ge_2$.

Chemical formula	**$UFe_{0.4}Ge_2$**
Formula weight (g mol^{-1})	206
Crystal system	Orthorhombic
Space group	*Cmcm* (No. 63)
Lattice parameters (Å)	*a*=4.083(5), *b*=15.805(5) *c*=4.030(5)
Cell volume ($Å^3$)	260.1(1)
Formula per unit cell (*Z*), Calculated density (gcm^{-3})	8, 10.5
Radiation, Wavelenght (Å)	Mo Kα, 0.71073
θ range (º)	2.6-42.1
Data set	$-5 \le h \le 7$, $-29 \le k \le 29$, $-5 \le l \le 7$
Collected / Unique reflections / R_{int}	3603/554/0.146
Refined parameters	19
Final agreement factors ($I>2\sigma(I)$) R, ωR_2	0.045, 0.117
Goodness of the fit	1.069
Extinction coefficient	0.0143
Highest/lowest peak of electron density (e-/$Å^3$)	8.265/-8.135

Table 11– Atomic coordinates and isotropic displacement parameters (U_{eq}) and their estimated standard deviations for $UFe_{0.4}Ge_2$.

Atom	Site	*x*	*y*	*z*	Occupation	U_{eq} (Å^2)
U	4*c*	0	0.3958(4)	1/4	1	0.0134(8)
Fe	4*c*	0	0.1916(5)	1/4	0.4	0.0353(8)
Ge1	4*c*	0	0.0529(0)	1/4	1	0.0129(8)
Ge2	4*c*	0	0.7501(0)	1/4	1	0.0301(0)

Table 12 – Selected interatomic distances for $UFe_{0.4}Ge_2$.

Atom pair		Distance (Å)	Atom pair		Distance (Å)
U	4Ge1	2.981(8)	Fe	1Ge1	2.191(7)
	2Ge2	3.062(8)		2Ge2	2.216(6)
	2Ge2	3.077(2)		2Ge2	2.242(6)
	4Fe	3.183(1)		4U	3.183(1)
	2Ge1	3.215(8)		1U	3.228(6)
	1Fe	3.228(6)			
	2U	3.863(9)			
Ge1	1Fe	2.191(7)	Ge2	2Fe	2.216(6)
	2Ge1	2.618(7)		2Fe	2.242(6)
	4U	2.981(8)		4Ge2	2.868(8)
	2U	3.215(8)		2U	3.062(8)
				2U	3.077(8)

Highlights

- Isothermal section of the U-Fe-Ge at 900ºC was investigated.
- Ten ternary compounds and four significant solubility ranges were found.
- Three new compounds and a solid solution were discovered.